JOURNAL OF VIROLOGY, Apr. 1997, p. 3228–3235 Vol. 71, No. 4
0022-538X/97/$04.00+0

Inducible Nitric Oxide Synthase in Theiler's Murine Encephalomyelitis Virus Infection

EMILIA L. OLESZAK,[1,2,3]* CHRISTOS D. KATSETOS,[4] JACEK KUZMAK,[1,2] AND ARUN VARADHACHARY[4]

Fels Institute for Cancer Research and Molecular Biology[1] and Departments of Biochemistry,[2] Neurology,[3] and Microbiology and Immunology,[4] Temple University School of Medicine, Philadelphia, Pennsylvania

Received 19 November 1996/Accepted 10 January 1997

We investigated the role of inducible nitric oxide synthase (iNOS) in Theiler's murine encephalomyelitis virus (TMEV) infection of susceptible (SJL) and resistant (C57BL/6 [B6]) strains of mice. TMEV is an excellent model of virus-induced demyelinating disease, such as multiple sclerosis (MS). Previous studies of others have suggested that NO may play a role in the pathogenesis of demyelinating disease. The presence and level of iNOS were determined in the brains and spinal cords of SJL and B6 TMEV-infected mice by the following methods: (i) PCR amplification of iNOS transcripts, followed by Southern blotting with an iNOS-specific probe, and (ii) immunohistochemical staining with an anti-iNOS-specific affinity-purified rabbit antibody. iNOS-specific transcripts were determined in the brains and spinal cord of both SJL and B6 TMEV-infected mice on days 0 (control), days 3, 6, and 10 (encephalitic stage of disease), and days 39 to 42, 66, and 180 (demyelinating phase) postinfection (p.i.). iNOS-specific transcripts were found in the brains and spinal cords of both SJL and B6 TMEV-infected mice at 6, 10, and 39 (SJL) days p.i., but they were absent in mock-infected mice and in TMEV-infected SJL and B6 mice at 0, 3, 66, and 180 days p.i. Immunohistochemical staining confirmed the presence of iNOS protein in both TMEV-infected SJL and B6 mice at days 6 and 10 p.i., but not at days 0, 3, 66, and 180 days p.i. Weak iNOS staining was also observed in TMEV-infected SJL mice at 42 days p.i. iNOS-positive staining was found in reactive astrocytes surrounding areas of necrotizing inflammation, particularly in the midbrain. Weak iNOS staining was also observed in cells of the monocyte/macrophage lineage in areas of parenchymal inflammation and necrosis (mesencephalon) and in leptomeningeal and white matter perivascular infiltrates of the spinal cord. Rod-shaped microglia-like cells and foamy macrophages (myelin-laden) were iNOS negative. These results suggest that NO does not play a direct role in the late phase of demyelinating disease in TMEV-infected mice.

Nitric oxide (NO) is a short-lived, highly reactive molecule with free radical properties (52, 58). NO production results from the conversion of L-arginine to L-citrulline by NO synthase (NOS) (52, 53, 77). The NO enzyme family consists of three isoforms: neuronal constitutive NOS (type I NOS), inducible NOS (iNOS or type II NOS), and endothelial constitutive NOS (type III NOS) (30, 52). iNOS expression is induced by lipopolysaccharide or cytokines, such as gamma interferon (IFN-γ) or interleukin 1β (IL-1β), and is calcium independent (8, 13, 15, 18, 29, 42, 50, 72). The NO generated by iNOS is the primary form of NO in acute and chronic inflammation, while rather lower concentrations of NO are released by constitutive expressed NOS (types I and III), which act as second messengers in NO signaling pathways in the neuronal and cardiovascular systems. NO exhibits toxic, cytostatic, and regulatory functions (3, 6, 9, 12, 23, 25, 33–36, 54, 65, 75, 76). It inhibits T-cell proliferation, and it plays a role in the antitumor and antimicrobial functions of the immune system (24, 32, 37, 41, 59, 73, 74). However, type II NOS-directed NO production is reported to be a potent neurotoxin and at least in vitro mediates tumor necrosis factor alpha (TNF-α) toxicity toward oligodendrocytes (20, 54, 57). Therefore, NO produced by iNOS may be both friend and foe. In the central nervous system (CNS), cytokine-induced iNOS is expressed mainly by macrophages, microglial cells, and astrocytes, but not by oligodendrocytes (11, 26, 29, 43, 55, 71, 78).

iNOS-derived NO has been detected in several inflammatory diseases of the CNS, such as experimental allergic encephalomyelitis (EAE) and viral encephalitis, induced experimentally in rodents by Borna virus, rabies virus, and herpes simplex virus (17, 21, 31, 38). It is not known whether NO plays a role in demyelination, which is seen in certain forms of EAE, or whether NO is associated only with the encephalitic stage of the disease.

In this report we investigated whether iNOS is expressed in the CNSs of mice infected with Theiler's murine encephalomyelitis virus (TMEV). This virus induces a biphasic disease in sensitive strains of mice (such as SJL) (45, 46, 61, 64, 68). The early phase of the disease is characterized by acute polioencephalomyelitis (early acute disease), in which the virus replicates mainly in neurons and to a lesser extent in astrocytes, macrophages, and microglia (10, 45, 47, 48). There are prominent neuronophagia and a characteristic intense mononuclear cell infiltration of neurons in the cerebral cortex and anterior horn cells of the spinal cord. A few weeks later, mice from susceptible strains develop the second phase of the disease, which is characterized by chronic demyelination associated with heavy mononuclear infiltration (late demyelinating disease). Pathological changes are limited to the spinal cord. During chronic demyelinating disease, most of the TMEV antigens can be detected in macrophages, astrocytes, and oligodendrocytes (10, 63, 68). It has been suggested that demyelination in TMEV-infected animals is mediated by the immune system (63). In contrast, resistant strains of mice

* Corresponding author. Mailing address: Fels Institute for Cancer Research and Molecular Biology, Temple University School of Medicine, 3420 N. Broad St., Philadelphia, PA 19106. Phone: (215) 707-7657. Fax: (215) 829-1320.

(C57BL/6 [B6]) develop only the acute phase of the disease, clear the virus, and do not develop demyelinating disease. TMEV infection of susceptible and resistant strains of mice offers a unique opportunity to study the role of NO in encephalitis and demyelination.

MATERIALS AND METHODS

Virus. The wild-type Daniel strain of TMEV was used in all experiments. The origin and propagation of this virus have been described previously (46, 47, 62).

Animals. Five- to six-week-old female SJL and B6 mice were purchased from Jackson Laboratory (Bar Harbor, Maine). Mice were housed in microisolators in an individual biohazard unit in a biohazard level II facility. All manipulations and changing of cages were performed in a biohazard hood. Mice were maintained in accordance with the standards of the American Association for Accreditation of Laboratory Animal Care. Sentinel mice were housed together with TMEV-infected mice and examined for the presence of a large number of common mouse pathogens (viruses and mycoplasma). No pathogens were detected. Mice were slightly anesthetized with methoxyflurane (Pitman-Moore, Mundelein, Ill.) and inoculated with 10^5 PFU of TMEV in a 20-μl volume in the right cerebral hemisphere. Control, mock-infected animals were injected with Dulbecco's modified Eagle medium containing 2% fetal calf serum and standard amounts of penicillin, streptomycin, and glutamine. Medium of identical composition was used to grow TMEV. At days 0, 3, 6, 10, 39, 42, 66 or 67, and 180 (SJL only) p.i., three to five SJL or B6 mice per group were euthanized by the administration of an overdose of methoxyflurane, and their spinal cords and brains were immediately removed and were either snap frozen in liquid nitrogen for RNA isolation or embedded in OCT compound (Tissue-Tech; Sakura, Torrance, Calif.) and stored in −80°C. Also, tissue specimens were placed in buffered formalin.

Histopathology and immunohistochemistry. Spinal cords and brains were embedded in paraffin, cut into 5-μm-thick sections, and stained with hematoxylin and eosin for light microscopy. iNOS was detected by immunohistochemistry, using an affinity-purified rabbit anti-iNOS antibody (Transduction Laboratories, Lexington, Ky.), according to the manufacturer's recommendations. Glial fibrillary acidic protein (GFAP) was detected by a similar approach, as previously described (60), using a rabbit anti-GFAP antibody (DAKO, Carpinteria, Calif.). Briefly, the slides were rehydrated in xylene and alcohols, the sections were washed with phosphate-buffered saline, and endogenous peroxidase was blocked by incubation for 30 min in 1.2% hydrogen peroxide in cold methanol. Alternatively, 5-μm-thick frozen sections were fixed for 10 min in cold acetone and stained by the procedures described above. Sections were incubated with goat serum for 45 min to reduce nonspecific binding. iNOS was detected by an immunoperoxidase technique (ABC kit; Vector Laboratories, Burlingame, Calif.). Sections were incubated with either anti-iNOS (1.25 μg/ml) or anti-GFAP antibody (diluted 1:1,000) for 1 h. Antigen-antibody complexes were detected with an anti-rabbit–biotinylated avidin–horseradish peroxidase complex according to the manufacturer's instructions. The sections were stained with 3,3′-diaminobenzidine as the substrate and then counterstained with Mayer's hematoxylin (Sigma Chemical Co., St. Louis, Mo.). Controls included normal rabbit immunoglobulin G (IgG) (1.25 μg/ml), which was used instead of a specific rabbit anti-iNOS or anti-GFAP antibody. Staining with control normal rabbit IgG was always negative.

RT-PCR and Southern blot analysis of iNOS mRNA in the brain and spinal cord. Total RNA was isolated from brain and spinal cord tissue of individual mice separately, using the RNA isolation kit of Stratagene (La Jolla, Calif.). The first strand of cDNA was synthesized by reverse transcriptase (RT) (Promega, Madison, Wis.) with 5 μg of starting RNA. The reaction was stopped by heating the mixture at 100°C for 10 min. cDNA was amplified by using primers selected from the iNOS cDNA (38) as follows: iNOS antisense 30-mer, 5′-GTCGACG AGCCTCGTGCTTTGGGCTCCTC-3′; and iNOS sense 30-mer, 5′-GTCGAC CTTCCGAAGTTTCTGGCAGCAGCG-3′. Amplification was performed as follows: 35 cycles of amplification, with 1 cycle consisting of three steps, namely, denaturation at 94°C for 45 s, primer annealing at 50°C for 90 s, and primer extension at 72°C for 3 min, followed by a final elongation step for 10 min at 72°C. β-Actin primers (Clontech, Palo Alto, Calif.) were used as controls to ensure the integrity of RNA. Hybridizations and Southern blotting were performed as described, using an iNOS-specific 30-mer hybridization probe, 5′-AC GTTCAGGACATCCTGCAAAAGCAGCTGG-3′.

RESULTS

To elucidate whether iNOS is expressed in the CNS of mice infected with TMEV, we have investigated the presence of iNOS transcripts by RT-PCR and the presence of iNOS protein by immunohistochemical staining. Susceptible (SJL) and resistant (B6) mice were infected intracerebrally with TMEV and euthanized at days 0, 3, 6, 10, 39, 42, 66 or 67, and 180 (SJL only) p.i. Control mice were injected intracerebrally with medium alone, as described in Materials and Methods, and they were sacrificed 6 and 39 days p.i. The presence of iNOS transcripts and iNOS protein were determined in the brains and spinal cords of all mice, as described in Materials and Methods. In addition, two or three animals from the TMEV-infected group were euthanized at the same time points listed above,

TABLE 1. Histopathology[a] and iNOS in TMEV-infected mice

Strain	No. of days p.i.	Brain			Leptomeningeal infiltrates[e]	Poliomyelitis[e]	Spinal cord		
		Encephalitis[b]	iNOS transcripts[c]	iNOS staining[d]			Vacuolar changes or demyelination[f]	iNOS transcripts	iNOS staining
SJL	3	−	Absent	Negative	−	−	−	Absent	Negative
	6	++	Present[g]	Strongly positive	+	++	+	Present[g]	Strongly positive
	10	+++	Present[g]	Strongly positive	++	+	−	Present[g]	Strongly positive
	39–42	+	Present[h]	Weakly positive	++	−	+++	Present[h]	Weakly positive
	66	+	Absent	Negative	++	−	+++	Absent	Negative
	180	−	Absent	Negative	++	−	+++	Absent	Negative
B6	3	+	Absent	Negative	+	−	−	Absent	Negative
	6	++	Present[g]	Strongly positive	+	++	+	Present[g]	Strongly positive
	10	++	Present[g]	Strongly positive	−	+	−	Present[g]	Strongly positive
	42	−	ND	Negative	−	−	−	ND	Negative
	67	−	Absent	Negative	−	−	−	Absent	Negative

[a] Histopathological changes in the brain (encephalitis) and spinal cord (leptomeningeal infiltrates, poliomyelitis, and vacuolar changes or demyelination) were measured.

[b] Symbols: −, unremarkable; +, mild leptomeningeal inflammation (no parenchymal inflammation and no necrosis); ++, moderate to severe inflammation with or without necrosis; +++, severe inflammation with overt necrosis.

[c] PCR and Southern blotting were carried out as described in Materials and Methods. ND, not determined.

[d] iNOS staining was determined by immunohistochemistry as described in Materials and Methods. iNOS staining was categorized as follows: negative, no staining; strongly positive, robust staining of tissue; weakly positive, weak staining.

[e] Symbols: −, unremarkable (for leptomeningeal infiltrates) or no infiltrates (for poliomyelitis); +, scant mononuclear infiltrates; ++, multifocal, nodular aggregates of inflammatory cells.

[f] Symbols: −, no vacuolar changes or demyelination; +, focal change involving one white matter funiculus only; +++, pronounced change, involving one or more funiculi.

[g] The level of iNOS transcripts in the brain was higher than that in the spinal cord.

[h] The level of iNOS transcripts in the brain was lower than that in the spinal cord.

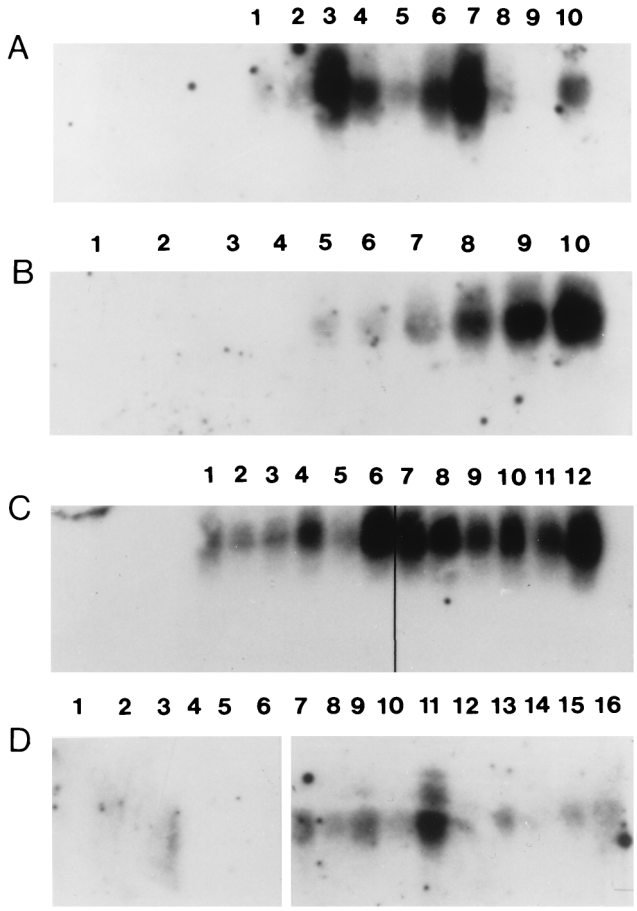

FIG. 1. iNOS transcripts in the CNSs of TMEV-infected and mock-infected mice. Results from individual mice are shown in each lane. (A) iNOS transcripts in the brains (lanes 1 to 5) and spinal cords (lanes 6 to 10) of TMEV-infected SJL mice at 6 day p.i. (B) iNOS transcripts in mock-infected (lanes 1 to 4) or TMEV-infected (lanes 5 to 10) B6 mice at 6 days p.i. iNOS transcripts in spinal cords (lanes 1, 3, 5, 6, and 7) and in brains (lanes 2, 4, 8, 9, and 10) are shown. (C) iNOS transcripts in TMEV-infected SJL (lanes 1 to 6) and TMEV-infected B6 (lanes 7 to 12) mice at 10 days p.i. iNOS transcripts in spinal cords (lanes 1, 3, 5, 7, 9, and 11) and brains (lanes 2, 4, 6, 8, 10, and 12) are shown. (D) iNOS transcripts in mock-infected (lanes 1 to 6) and TMEV-infected (lanes 7 to 16) SJL mice at 39 days p.i. iNOS transcripts in spinal cords (lanes 1, 3, 5, 7 to 9, 10, and 11) and in brains (lanes 2, 4, 6, 12 to 15, and 16) are shown.

and brains and spinal cords were processed individually for hematoxylin-and-eosin histological evaluation of pathology.

Expression of iNOS in early acute disease. None of the TMEV-infected animals showed overt clinical signs of encephalitis, although histological analyses revealed polioencephalomyelitis at days 6 and 10 p.i. (Table 1). SJL mice showed more severe gray matter disease on day 10 p.i. than B6 mice (Table 1). However, B6 mice showed inflammatory infiltrates in the CNS earlier than SJL mice. We have detected high levels of iNOS transcripts in the brain and spinal cord in both strains of mice. Little or no detectable iNOS expression was found in the brain and spinal cord at day 3 p.i. (data not shown). In contrast, the level of expression of iNOS transcripts was significant at days 6 and 10 p.i. in both susceptible and resistant strains of mice (Fig. 1A, B, and C). At 6 days p.i., a certain fluctuation was observed in the levels of iNOS transcripts in the CNS of individual TMEV-infected SJL mice (Fig. 1A). Similar fluctuations in the levels of iNOS transcripts have been reported by others (38) for virus-induced encephalitis. The induction of iNOS mRNA on days 6 and 10 p.i. coincided with the severity of polioencephalomyelitis (Table 1). In general, higher levels of iNOS expression were detected in the brains of SJL and B6 mice than in the spinal cords during early acute disease (Fig. 1A and C). iNOS transcripts were not detected by RT-PCR, followed by Southern blotting, in the brains or spinal cords of mock-infected mice at 6 or 39 day p.i. (Fig. 1B and D), in agreement with the findings of others (55, 56).

Using antibodies to iNOS protein and immunohistochemical staining, we have identified the CNS cells that expressed iNOS. At days 6 and 10 p.i., cells that stained positive with iNOS antibody were identified in areas of intense inflammation in both TMEV-infected SJL and B6 mice. In the brains of both strains of mice, these cells included predominantly reactive astrocytes (Fig. 2A and B and 3A and B), cells of the monocyte/macrophage lineage, and hypertrophic endothelial cells in areas of active vascular ingrowth (Fig. 2C and D and 3B). Rare perivascular monocyte-like cells of the leptomeningeal infiltrates were also iNOS positive (Fig. 3C), whereas morphologically overt lymphocytes were as a rule iNOS negative. Normal interfascicular fibrous and protoplasmic astrocytes, Bergmann's glia, as well as oligodendrocytes, were iNOS negative. Similarly, no staining was observed in normal endothelial or smooth muscle cells. To confirm the identity of the cells that expressed the iNOS protein, we stained adjacent sections either with anti-GFAP antibody (Fig. 2A and 3A) or with anti-iNOS antibody (Fig. 2B and 3B). Cells which were positive for iNOS were also stained with anti-GFAP antibody. Thus, reactive astrocytes represent the major cell type that expressed iNOS protein in the brains of TMEV-infected mice. This is in contrast to the lack of iNOS reactivity in normal astroglia. iNOS protein was not detected by immunohistochemical staining in the brains of uninfected, unmanipulated SJL and B6 mice with the rabbit anti-mouse iNOS polyclonal antibody previously described (data not shown).

The profile of iNOS staining in the spinal cord was similar to that described for the areas of encephalitis. At 6 and 10 days p.i., reactive astrocytes near areas of inflammation were iNOS positive. Occasional or scattered iNOS-positive cells of the macrophage/monocyte type were detected in foci of spinal meningitis and in spinal gray matter infiltrates. However, rod-shaped microglia-like cells were consistently negative (Fig. 3D). There was no difference in the distribution of iNOS-positive cells in the CNS of TMEV-infected SJL or B6 mice.

Expression of iNOS in late demyelinating disease. At day 39 p.i., which corresponds to the beginning of demyelinating disease (Fig. 1D), iNOS transcripts were detected in the spinal cords of five TMEV-infected SJL mice. Lower levels of iNOS message were detected in the brains of these mice. However, iNOS transcripts could not be detected in the brains and spinal cords of TMEV-infected susceptible SJL mice with extensive demyelinating disease 66 and 180 days p.i. (Fig. 4). Also, at 67 days p.i., iNOS transcripts could not be detected in the brains and spinal cords of TMEV-infected resistant B6 mice that were free of demyelinating disease (Fig. 4). β-Actin transcripts were amplified from each brain and spinal cord cDNA to ensure the integrity of RNA (Fig. 4). Lack of iNOS expression in the brain or spinal cord at this time point was confirmed by the lack of any immunohistochemical staining with anti-iNOS antibody in both SJL and B6 mice (Fig. 2G and 3E and F and data not shown). Foamy (myelin-laden) macrophages in areas of demyelination in the spinal cords of SJL mice 67 days p.i. were not stained with anti-iNOS antibody (Fig. 2G). At days 42 and 67 p.i., we did not detect any pathological changes in the brains and spinal cords of B6 mice (Fig. 3E and F and data not shown). In contrast, prominent inflammatory infiltrates, pro-

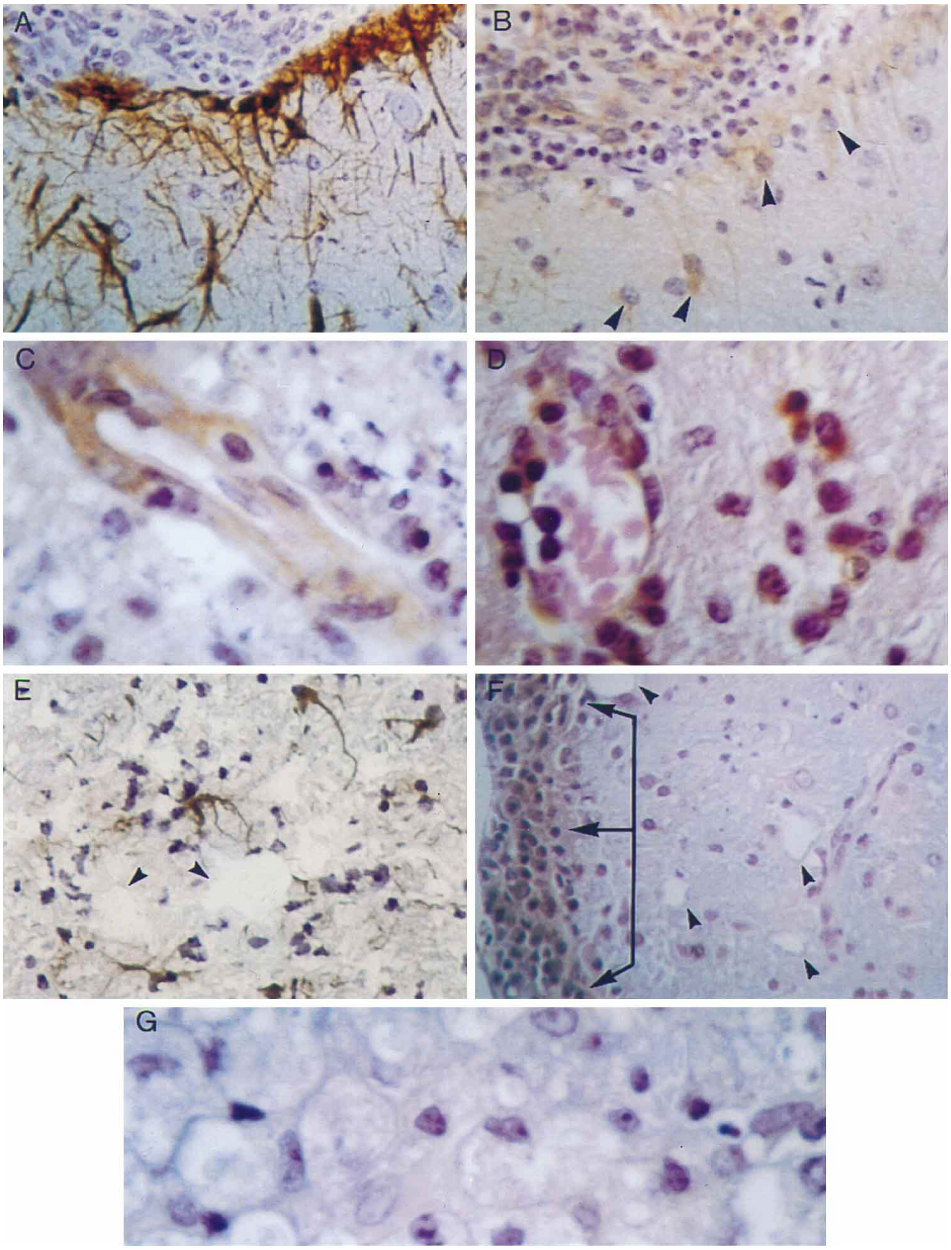

FIG. 2. Immunocytochemical detection of GFAP (A) and iNOS protein (B to G) in the CNS of SJL mice at 10 (A to C), 6 (D), 42 (E and F), and 66 (G) days p.i. With the exception of panel E (frozen section), all staining was performed on paraffin-embedded tissue sections. (A) Phase of encephalitis and poliomyelitis of SJL mice 10 days p.i. An area of intense leptomeningeal inflammation surrounding midbrain parenchyma, where a brisk, reactive (principally subpial) astrocytic meshwork shows strong filamentous GFAP staining in glial perinuclear cytoplasm and fibrillary processes, is shown. Compare this with the lack of GFAP staining in mononuclear infiltrates involving the subarachnoid space (top portion of photomicrograph). Original magnification, ×400. (B) Same field as in panel A from an adjacent paraffin-embedded section immunostained for iNOS. Diffuse iNOS-like staining is present in reactive subpial astrocytes (arrowheads) and also in occasional monocyte/macrophage cells in the leptomeningeal infiltrate (top portion of photomicrograph). Original magnification, ×400. (C) Phase of encephalitis and poliomyelitis of SJL mice 10 days p.i. A high-magnification view of an area of intense (necrotizing) inflammation involving the mesencephalic-diencephalic region is shown. Note iNOS-like localization in hypertrophic endothelial cells representative of active vascular ingrowth (neovascularization). Also, note karyorrhectic debris denoting parenchymal necrosis, adjacent to the vessel. Original magnification, ×1,000. (D) Phase of encephalitis and poliomyelitis of SJL mice 6 days p.i. A high-magnification view of an area of spinal cord gray matter inflammation involving one of the posterior horns in the thoracic region. There is iNOS-like staining in perivascular inflammatory cells of the monocyte/macrophage lineage and in vascular endothelial cells. Original magnification, ×1,000. (E) Early phase of spinal cord demyelination of SJL mice 42 days p.i. A lateral column and thoracic cord are shown. Numerous iNOS-immunoreactive fibrillary astrocytes are present between inflammatory cells in a background of incipient vacuolar change (arrowheads) suggestive of early demyelination. Original magnification, ×400. (F) Phase of spinal cord demyelination of SJL mice 42 days p.i. Focal, weak, and ill-defined iNOS-like immunoreactivity is detected among leptomeningeal infiltrates (the three arrows) encroaching upon the lateral white matter funiculus of the spinal cord (thoracic level). Note vacuolar change (arrowheads) in the neuropil of the lateral column. Original magnification, ×400. (G) Phase of spinal cord demyelination of SJL mice 66 days p.i. An area of overt demyelination involving the posterior white matter funiculus (thoracic level) is shown. The section is immunostained for iNOS. There is no iNOS staining in large foamy (myelin-laden) macrophages that typify these full-blown demyelinating lesions. Original magnification, ×1,000.

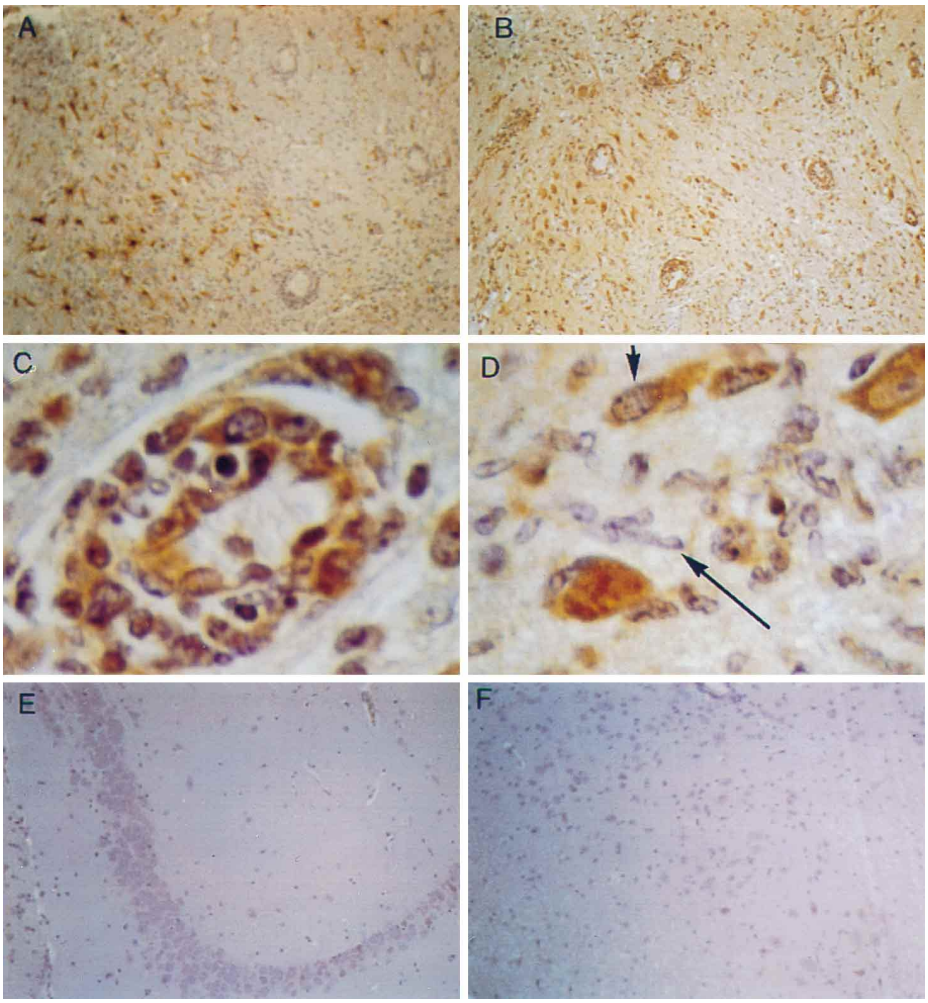

FIG. 3. Immunohistochemical detection of GFAP (A) and iNOS protein (B to F) in the CNSa of B6 mice at 6 (A to D) and 42 (E and F) days p.i. (A) Phase of encephalitis and poliomyelitis of B6 mice 6 days p.i. An area of intense parenchymal inflammation (encephalitis) involving the mesencephalic-diencephalic region is shown. Briskly proliferating reactive astrocytes exhibit strong GFAP staining. There is no staining in blood vessels and in mononuclear infiltrates in the Virchow-Robin spaces (perivascular cuffs). Original magnification, ×100. (B) Same field as in panel A, from an adjacent paraffin-embedded section immunostained for iNOS. There is widespread iNOS-like immunoreactivity involving reactive astrocytes, blood vessels (particularly endothelial cells), and subpopulations of mononuclear infiltrates most compatible with cells of the monocyte/macrophage lineage. Original magnification, ×100. (C) Phase of encephalitis and poliomyelitis of B6 mice 6 days p.i. Transmural and perivascular inflammatory cell aggregates from a focus of necrotizing encephalitis involving the diencephalic-mesencephalic region. Robust iNOS staining is present in monocyte/macrophage cells traversing the vessel wall and in the Virchow-Robin (perivascular) space. Also, note iNOS localization in endothelial cells of the inflamed vessel (vasculitis). Original magnification, ×1,000. (D) Phase of encephalitis and poliomyelitis of B6 mice 6 days p.i. A focus of poliomyelitis similar to that depicted in panel C is shown. Robust iNOS-like immunoreactivity is present in a reactive astrocyte (short arrow). Compare with lack of iNOS staining in adjoining rod-shaped microglia-like cells (long arrow). Original magnification, ×1,000. (E) B6 mice 42 days p.i. There is no evidence of iNOS staining in the hippocampus. Original magnification, ×100. (F) Cerebral section of a B6 mouse infected with TMEV 42 days p.i. and immunostained for iNOS. Absence of iNOS staining in this field from the diencephalic-mesencephalic region. Original magnification, ×100. A similar lack of immunoreactivity was noted in sections of the spinal cord (data not shown).

nounced demyelination, and reactive astrocytes could be demonstrated in the spinal cords of TMEV-infected SJL mice, while the brains were unremarkable (Table 1). These results demonstrate that inflammatory infiltrates and gliosis are not always associated with iNOS expression.

We have also examined the expression of iNOS at the terminal stage of demyelinating disease in TMEV-infected SJL mice, approximately 6 months p.i. At this time point, mice lost their righting reflex, their hind limbs were paralyzed, and they became incontinent. We did not detect any iNOS message in the brains and spinal cords of SJL mice despite overt demyelination and inflammatory infiltration of the spinal cord (Fig. 4E and F). Similarly, iNOS was not detected using anti-iNOS antibody in reactive astrocytes and in foamy (myelin-laden) macrophages in areas of demyelination (spinal cord). Cells of the macrophage/monocyte lineage evident in perivascular cuffs were also negative (data not shown).

DISCUSSION

The mechanism of the pathogenesis of demyelinating disease, such as multiple sclerosis (MS), is poorly understood. It has been suggested that myelin and oligodendrocyte destruction in MS can be attributed to a direct attack of cytolytic T cells (1, 63, 69). In addition, $CD4^+$ T cells, macrophages, microglia, and astrocytes may participate in myelin destruction, either directly and/or indirectly by secreting cytokines, such as TNF-α and lymphotoxin (28, 58). In addition, it has been

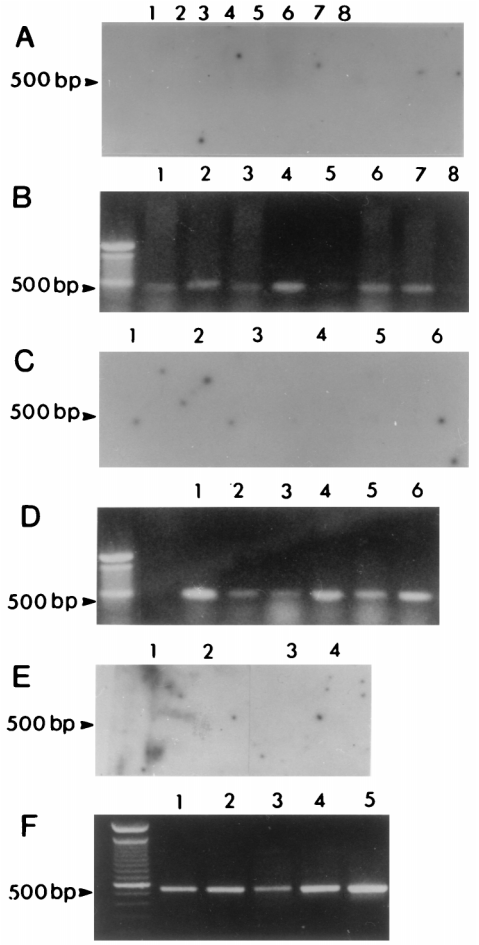

FIG. 4. iNOS transcripts could not be detected in the CNS of TMEV-infected resistant B6 mice at 67 days p.i. (A and B) or susceptible SJL mice at the late phase of demyelinating disease at 66 (C and D) and 180 (E and F) days p.i. Results from individual mice are shown in each lane. (A) Southern blot with an iNOS-specific probe of transcripts in the brains (lanes 1 to 4) and spinal cords (lanes 5 to 8) of TMEV-infected B6 mice at 67 days p.i. (B) Actin transcripts in the brains (lanes 1 to 4) and spinal cord (lanes 5 to 8) corresponding to the brains and spinal cords of TMEV-infected B6 mice described above for panel A. (C) Southern blot with an iNOS-specific probe of transcripts in the brains (lanes 1 to 3) and spinal cords (lanes 4 to 6) of TMEV-infected SJL mice at 66 days p.i. (D) Actin transcripts in the brains (lanes 1 to 3) and spinal cords (lanes 4 to 6) corresponding to the brains and spinal cords of TMEV-infected SJL mice described above for panel C. (E) Southern blot with an iNOS-specific probe of transcripts in the brains (lanes 1 and 3) and spinal cords (lanes 2 and 4) of TMEV-infected paralyzed SJL mice at 180 days p.i. (F) Actin transcripts in the brains (lanes 1 and 3) and spinal cords (lanes 2 and 4) corresponding to the brains and spinal cords of TMEV-infected SJL mice described above for panel E. Control actin transcript (Clontech) is shown in lane 5.

proposed that NO may mediate neuron and oligodendrocyte death and may participate in demyelination (9, 31, 38, 56). NO is a neurotransmitter in the CNS, which is constitutively produced by type I NOS in neurons (66). Type II NOS (iNOS) can be found in activated astrocytes, macrophages, microglia, and neurons (7, 9, 12, 21, 26, 29, 40, 55–57), while type III NOS is found in endothelial cells, a subset of neurons of the hippocampus and astrocytes of the CNS (2, 20). Astrocytes and microglial cells express iNOS in response to endotoxin and to cytokines such as TNF-α, IFN-γ, and IL-1β (8, 13, 15, 42, 50). In a few in vitro studies, it has been demonstrated that NO may mediate the destruction of oligodendrocytes (54, 57). NO toxicity can be attributed to the nitrosylation of target iron-sulfur proteins, including key enzymes necessary for DNA replication and repair, or mitochondrial energy production (44, 65, 66, 75, 76). Direct mitochondrial damage has been detected in oligodendrocytes treated with *S*-nitroso-*N*-acetyl-DL-penicillamine, a NO-releasing chemical. In addition, NO may react with the superoxide anion to form peroxynitrite ($ONOO^-$) (4, 49, 78), which induces lipid peroxidation. Membrane peroxidation as well as swollen oligodendrocyte cell bodies, has been demonstrated in the brains of patients with MS, which supports the hypothesis that NO may mediate oligodendrocyte damage. Furthermore, growing lesions in MS patients are surrounded by infiltrates of activated macrophages and microglia, which produce TNF-α, a potent inducer of NO. Recently, it was reported that iNOS mRNA can be detected in microglia and/or astrocytes of patients with MS (1, 7). Therefore, NO may be directly involved in the demyelinating process. Increased levels of iNOS have also been demonstrated in EAE, which mimics certain aspects of MS (17, 38), and in astrocytes of mouse hepatitis virus-infected animals with chronic demyelinating disease (67).

With the objective of determining whether NO plays a role in the pathogenesis of inflammatory and/or demyelinating disease, we have studied iNOS in TMEV infection. TMEV induces a biphasic disease in susceptible strains of mice (14, 68). The early disease resembles polioencephalomyelitis and is followed several weeks later by late chronic demyelination of the spinal cord (47, 48). In contrast, resistant strains of mice develop only gray matter disease, clear the virus, and do not develop demyelination. Both acute and chronic demyelinating disease is characterized by mononuclear cell infiltrates. During late demyelinating disease, extreme meningeal and perivascular mononuclear cell infiltrates are found in susceptible SJL mice with concomitant demyelination in the spinal cord (46). Using this model of virus-induced demyelinating disease (19, 64), we were able to study separately the induction of iNOS at both the encephalitic and demyelinating phases of the disease. We have demonstrated high levels of NO produced in the brains and spinal cords of both resistant and susceptible strains of mice during early gray matter disease. The highest level of iNOS was observed at days 6 and 10 p.i. By immunohistochemical staining with a polyclonal anti-iNOS antibody, we have identified reactive astroglia and cells of the macrophage or microglia lineage as the cells that expressed iNOS protein in the brains and spinal cords of both strains of mice. It remains to be determined whether cells of the macrophage or microglia lineage, which expressed iNOS in the CNS, were part of inflammatory infiltrates coming from the periphery or were activated resident CNS cells. iNOS transcripts and low levels of iNOS protein were detected in TMEV-infected SJL mice at 39 days p.i., at the beginning of the demyelinating phase of the disease. However, despite pronounced demyelination and fulminant mononuclear infiltration of the spinal cords of TMEV-infected SJL mice at 66 and 180 days p.i., iNOS transcripts could not be detected. Similarly, immunohistochemical staining confirmed the absence of iNOS-expressing cells in the spinal cords of these mice. iNOS transcripts were not detected in the brains or spinal cords of mock-infected mice. This is in agreement with reports of others (55, 56), who did not find iNOS transcripts in neurons of mock-infected mice. Therefore, we demonstrated the presence of iNOS mRNA and iNOS protein in the brains and spinal cords of both susceptible and resistant strains of mice infected with TMEV, but only during early gray matter disease. In contrast, both iNOS transcripts and iNOS protein were absent at 60 and 180 days p.i. from the CNSs of B6 and SJL mice, although SJL mice showed severe progressive demyelination and inflammatory lesions.

Our results suggest that at least in TMEV-induced demyelinating disease, NO is not involved in the late phase of demyelinating disease. The significance of iNOS expression during acute gray matter disease in both SJL and B6 mice is not well understood, although it has been reported for other acute viral infections of the CNS. It has been reported that NO produced during acute viral infections actually inhibits viral replication of poxvirus, herpesvirus, coxsackievirus, and rhabdovirus but not flavivirus (5, 16, 35, 39, 51). Inhibition of replication of DNA viruses by IFN-γ-induced iNOS has been attributed to the inhibition by NO of ribonucleotide reductase, an enzyme that play a role in viral DNA synthesis (35, 44) or deamination of viral DNA (75). The mechanism of inhibition of RNA virus replication (such as vesicular stomatitis virus or coxsackie B3 virus) by NO is less understood. NO may play a neuroprotective role in virus-induced diseases of the CNS by inhibiting viral replication. On the other hand, treatment of mice infected with lymphocytic choriomeningitis virus (11) or Sindbis virus (70) with inhibitors of iNOS or NOS, respectively, resulted in enhancement of severity of clinical symptoms and decreased the survival of infected animals, without affecting replication of the virus in the CNS. The protective effect of NO in Sindbis virus-induced encephalitis has been attributed to the enhancement of the ability of neurons to survive viral infection by modification or induction of new protein(s), until a specific immune response can be mounted (70). On the other hand, NO induced by certain neurotropic viruses may contribute to the pathogenesis of the infection, as has been demonstrated for Borna disease virus or flavivirus-induced encephalitis (38, 39). Treatment of tick-borne encephalitis virus-infected mice with aminoguanidine (an inhibitor of iNOS) increased their survival. Thus, NO may play an antiviral, neuroprotective, or neurotoxic role in viral infections of the CNS. Experiments using specific inhibitors of iNOS, such as aminoguanidine (27), should help determine whether NO can affect replication of TMEV.

ACKNOWLEDGMENT

This work was supported in part by a grant to E.L.O. from the Eleanor Naylor Dana Charitable Trust.

REFERENCES

1. **Bagasra, O., F. H. Michaels, Y. M. Zheng, L. E. Bobroski, S. V. Spitsin, Z. F. Fu, R. Tawadros, and H. Koprowski.** 1995. Activation of the inducible form of nitric oxide synthase in the brains of patients with multiple sclerosis. Proc. Natl. Acad. Sci. USA **92:**12041–12045.
2. **Barna, M., T. Komatsu, and C. S. Reiss.** 1996. Activation of type III nitric oxide synthase in astrocytes following a neurotropic viral infection. Virology **223:**331–343.
3. **Beasley, D., J. H. Schwartz, and B. M. Breener.** 1991. Interleukin 1 induces prolonged L-arginine-dependent cyclic guanosine monophosphate and nitrite production in rat vascular smooth muscle cells. J. Clin. Invest. **87:**602–608.
4. **Beckman, J. S., and J. P. Crow.** 1993. Pathological implications of nitric oxide, superoxide and peroxynitrite formation. Biochem. Soc. Trans. **21:**330–334.
5. **Bi, Z., and C. S. Reiss.** 1995. Inhibition of vesicular stomatitis virus infection by nitric oxide. J. Virol. **69:**2208–2213.
6. **Bianco, F. J., R. L. Ochs, H. Schwarz, and M. Lotz.** 1995. Chondrocyte apoptosis induced by nitric oxide. Am. J. Pathol. **146:**75–85.
7. **Bö, L., T. M. Dawson, S. Wesselingh, S. Mörk, S. Choi, P. A. Kong, D. Hanley, and B. Trapp.** 1994. Induction of nitric oxide synthase in demyelinating regions of multiple sclerosis brains. Ann. Neurol. **36:**778–786.
8. **Bogdan, C., Y. Vodovotz, J. Paik, Q. W. Xie, and C. Nathan.** 1994. Mechanism of suppression of nitric oxide synthase expression by interleukin-4 in primary mouse macrophages. J. Leukocyte Biol. **55:**227–233.
9. **Boje, K. M., and P. K. Arora.** 1992. Microglia-produced nitric oxide and reactive nitrogen oxides mediate neuronal cell death. Brain Res. **587:**250–256.
10. **Brahic, M., W. G. Stroop, and J. R. Baringer.** 1981. Theiler's virus persists in glial cells during demyelinating disease. Cell **26:**123–128.
11. **Campbell, I. L.** 1996. Exacerbation of lymphocytic choriomeningitis in mice treated with the inducible nitric oxide synthase inhibitor aminoguanidine. J. Neuroimmunol. **71:**31–36.
12. **Chao, C. C., S. Hu, T. W. Molitor, E. G. Shaskan, and P. K. Peterson.** 1992. Activated microglia mediate neuronal cell injury via a nitric oxide mechanism. J. Immunol. **149:**2736–2741.
13. **Chesrown, S. E., J. Monier, G. Visner, and H. S. Nick.** 1994. Regulation of inducible nitric oxide synthase mRNA levels by LPS, IFN-γ, TGFβ, and IL-10 in murine macrophage cell lines and rat peritoneal macrophages. Biochem. Biophys. Res. Commun. **200:**126–134.
14. **Clatch, R. J., S. D. Miller, R. Metzner, M. C. Dal Canto, and H. L. Lipton.** 1990. Monocytes/macrophages isolated from the mouse central nervous system contain infectious Theiler's murine encephalomyelitis virus (TMEV). Virology **176:**244–254.
15. **Corradin, S. B., N. Fasel, Y. Buchmüller-Rouiller, A. Ransijn, J. Smith, and J. Manuel.** 1993. Induction of macrophage nitric oxide production by IFN-γ and TNF-α is enhanced by interleukin-10. Eur. J. Immunol. **23:**2045–2048.
16. **Croen, K. D.** 1993. Evidence for an antiviral effect of nitric oxide. Inhibition of herpes simplex virus type 1 replication. J. Clin. Invest. **91:**2446–2452.
17. **Cross, A. H., T. P. Misko, R. F. Lin, W. F. Hickey, J. L. Trotter, and R. G. Tilton.** 1994. Aminoguanidine, an inhibitor of inducible nitric oxide synthase, ameliorates experimental autoimmune encephalomyelitis in SJL mice. J. Clin. Invest. **93:**2684–2690.
18. **Cunha, F. Q., S. Moncada, and F. Y. Liew.** 1992. Interleukin-10 (IL-10) inhibits the induction of nitric oxide synthase by interferon-γ in murine macrophages. Biochem. Biophys. Res. Commun. **182:**1155–1159.
19. **Dal Canto, M. C., and H. L. Lipton.** 1977. Multiple sclerosis. Animal model: Theiler's virus infection in mice. Am. J. Pathol. **88:**497–500.
20. **Dawson, V. L., T. M. Dawson, E. D. London, D. S. Bredt, and S. H. Snyder.** 1991. Nitric oxide mediates glutamate neurotoxicity in primary cultures. Proc. Natl. Acad. Sci. USA **88:**6368–6371.
21. **Dighiero, P., I. Reux, J. J. Hauw, A. M. Fillet, Y. Courtois, and O. Goureau.** 1994. Expression of inducible nitric oxide synthase in cytomegalovirus-infected glial cells of retinas from AIDS patients. Neurosci. Lett. **166:**31–34.
22. **Dinerman, J. L., T. M. Dowson, M. J. Schell, A. Snowman, and S. H. Snyder.** 1994. Endothelial nitric oxide synthase localized to hypocampal pyrimidal cells: implication for synaptic plasticity. Proc. Natl. Acad. Sci. USA **91:**4214–4218.
23. **Dorheim, M. A., W. R. Tracey, J. S. Pollock, and P. Grammas.** 1994. Nitric oxide synthase activity is elevated in brain microvessels in Alzheimer's disease. Biochem. Biophys. Res. Commun. **205:**659–665.
24. **Eisenstein, T. K., D. Huang, J. J. Meissler, and B. Al-Ramadi.** 1994. Macrophage nitric oxide mediates immunosuppression in infectious inflammation. Immunobiology **191:**493–502.
25. **Fu, Y., and E. P. Blankenhorn.** 1992. Nitric oxide-induced anti-mitogenic effects in high and low responder rat strains. J. Immunol. **148:**2217–2222.
26. **Galea, E., D. J. Reis, and D. L. Feinstein.** 1994. Cloning and expression of inducible nitric oxide synthase from rat astrocytes. J. Neurosci. Res. **37:**406–414.
27. **Griffiths, M. J. D., M. Messent, R. J. MacAllister, and T. W. Evans.** 1993. Aminoguanidine selectively inhibits inducible nitric oxide synthase. Br. J. Pharmacol. **110:**963–968.
28. **Hauser, S. L., A. K. Bhan, F. Gilles, M. Kemp, C. Kerr, and H. L. Weiner.** 1986. Immunohistochemical analysis of the cellular infiltrate in multiple sclerosis lesions. Ann. Neurol. **19:**578–582.
29. **Hewett, S. J., J. A. Corbett, M. L. McDaniel, and D. W. Choi.** 1993. IFN-γ and IL-1β induce nitric oxide formation from primary mouse astrocytes. Neurosci. Lett. **164:**229–232.
30. **Hibbs, J. B., R. R. Taintor, Z. Vavrin, and E. M. Rachlin.** 1988. Nitric oxide: a cytotoxic activated macrophage effector molecule. Biochem. Biophys. Res. Commun. **157:**87–94.
31. **Hopper, D. C., S. T. Ohnishi, R. Kean, Y. Numagami, B. Dietzschold, and H. Koprowski.** 1995. Local nitric oxide production in viral and autoimmune diseases of the central nervous system. Proc. Natl. Acad. Sci. USA **92:**5312–5316.
32. **Ialenti, A., A. Ianaro, S. Moncada, and M. Di Rosa.** 1992. Modulation of acute inflammation by endogenous nitric oxide. Eur. J. Pharmacol. **211:**177–182.
33. **Isomura, K., O. Fukase, and H. Watanabe.** 1976. Cytotoxicities and mutagenicities of gaseous air pollutants on cultured cells. Taiki Osen Kenkyu **11:**59–64.
34. **Isomura, K., M. Chikahira, K. Teranshi, and K. Hamada.** 1984. Induction of mutations and chromosome aberrations in lung cells following in vivo exposure of rats to nitrogen oxides. Mutat. Res. **136:**119–125.
35. **Karupiah, G., and N. Harris.** 1995. Inhibition of viral replication by nitric oxide and its reversal by ferrous sulfate and tricarboxylic acid cycle metabolites. J. Exp. Med. **181:**2171–2179.
36. **Kitajima, I., K. Kawahara, T. Nakajima, Y. Soejima, T. Matsuyama, and I. Maruyama.** 1994. Nitric oxide-mediated apoptosis in murine mastocytoma. Biochem. Biophys. Res. Commun. **204:**244–251.
37. **Kolb, H., and V. Kolb-Bachofen.** 1992. Nitric oxide: a pathogenic factor in autoimmunity. Immunol. Today **13:**157–160.

38. **Koprowski, H., Y. M. Zhen, E. Heber-Katz, N. Fraser, L. Rorke, Z. F. Fu, C. Hanlon, and B. Dietzschold.** 1993. In vivo expression of inducible nitric oxide synthase in experimentally induced neurologic diseases. Proc. Natl. Acad. Sci. USA **90:**3024–3027.
39. **Kreil, T. R., and M. M. Eibl.** 1996. Nitric oxide and viral infection: no antiviral activity against a flavivirus in vitro, and evidence for contribution to pathogenesis in experimental infection in vivo. Virology **219:**304–306.
40. **Krönke, K. D., K. Fehsel, K. Alsdorff, and V. Kolb-Bachofen.** 1994. Expression of inducible NO-synthase in human monocytes. Immunobiology **191:** 267–268.
41. **Kubes, P., M. Suzuk, and D. N. Granger.** 1991. Nitric oxide: an endogenous modulator of leukocyte adhesion. Proc. Natl. Acad. Sci. USA **88:**4651–4655.
42. **Lamas, S., T. Michel, B. M. Brenner, and P. A. Marsden.** 1991. Nitric oxide synthesis in endothelial cells: evidence for a pathway inducible by TNF-α. Am. J. Physiol. **261:**C634–C641.
43. **Lee, S. C., D. W. Dickson, W. Liu, and C. F. Brosnan.** 1993. Induction of nitric oxide synthase activity in human astrocytes by IL-1β and IFN-γ. J. Neuroimmunol. **46:**19–24.
44. **Lepoivre, M., F. Fieschi, J. Coves, L. Thelander, and M. Fontecave.** 1991. Inactivation of ribonucleotide reductase by nitric oxide. Biochem. Biophys. Res. Commun. **179:**442–448.
45. **Levy, M., C. Aubert, and M. Brahic.** 1992. Theiler's virus replication in brain macrophages cultured in vitro. J. Virol. **66:**3188–3193.
46. **Lindsley, M. D., and M. Rodriguez.** 1989. Characterization of the inflammatory response in the central nervous system of mice susceptible or resistant to demyelination by Theiler's virus. J. Immunol. **142:**2677–2682.
47. **Lipton, H. L.** 1975. Theiler's virus infection in mice: an unusual biphasic disease process leading to demyelination. Infect. Immun. **11:**1147–1155.
48. **Lipton, H. L.** 1978. Characterization of the TO strains of Theiler's mouse encephalomyelitis viruses. Infect. Immun. **20:**869–872.
49. **Lipton, S. A., Y. B. Choi, Z. H. Pan, S. Z. Lei, H. S. V. Chen, N. J. Sucher, J. Loscalzo, D. J. Singel, and J. S. Stamier.** 1993. A redox-based mechanism for the neuroprotective and neurodestructive effects of nitric oxide and related nitrosocompounds. Nature **364:**626–631.
50. **Lowenstein, C. J., E. W. Alley, P. Raval, A. M. Snowman, S. H. Snyder, S. W. Russell, and W. J. Murphy.** 1993. Macrophage nitric oxide synthase gene: two upstream regions mediate induction by interferon γ and lipopolysaccharide. Proc. Natl. Acad. Sci. USA **90:**9730–9734.
51. **Lowenstein, C. J., S. L. Hill, A. Lafond-Walker, J. Wu, G. Allen, M. Landavere, N. R. Rose, and A. Herskowitz.** 1996. Nitric oxide inhibits viral replication in murine myocarditis. J. Clin. Invest. **97:**1837–1843.
52. **Marlena, M. A.** 1993. Nitric oxide synthase structure and mechanism. J. Biol. Chem. **268:**12231–12234.
53. **Marletta, M. A., P. S. Yocr, R. Lyengar, C. D. Leaf, and J. S. Wishnok.** 1988. Macrophage oxidation of L-arginine to nitrite and nitrate: nitric oxide is an intermediate. Biochemistry **27:**8706–8711.
54. **Merrill, J. E., L. J. Ignarro, M. P. Sherman, J. Melinek, and T. E. Lane.** 1993. Microglial cell cytotoxicity of oligodentrocytes is mediated through nitric oxide. J. Immunol. **151:**2132–2141.
55. **Minc-Golomb, D., I. Tsarfaty, and J. P. Schwartz.** 1994. Expression of inducible nitric oxide synthase by neurones following exposure to endotoxin and cytokine. Br. J. Pharmacol. **112:**720–722.
56. **Minc-Golomb, D., G. Yadid, I. Tsarfaty, J. H. Resau, and J. P. Schwartz.** 1996. In vivo expression of inducible nitric oxide synthase in cerebellar neurons. J. Neurochem. **66:**1504–1509.
57. **Mitrovic, B., L. J. Ignarro, S. Montestruque, A. Smoll, and J. E. Merrill.** 1994. Nitric oxide as a potential pathological mechanism in demyelination: its differential effects on primary glial cells in vitro. Neuroscience **61:**575–585.
58. **Nathan, C., and Q. W. Xie.** 1994. Regulation of biosynthesis of nitric oxide. J. Biol. Chem. **269:**13725–13728.
59. **Nussler, A. K., and T. R. Billiar.** 1993. Inflammation, immunoregulation, and inducible nitric oxide synthase. J. Leukocyte Biol. **54:**171–178.
60. **Oleszak, E. L., G. Murdoch, L. Manuelidis, and E. E. Manuelidis.** 1988. Growth factor production by Creutzfeldt-Jacob disease cell lines. J. Virol. **62:**3103–3108.
61. **Oleszak, E. L., J. Kuzmak, R. A. Good, and C. D. Platsoucas.** 1995. Immunobiology of TMEV infection. Immunology of Theiler's murine encephalomyelitis virus infection. Immunol. Res. **14:**13–33.
62. **Oleszak, E. L., J. L. Leibowitz, and M. Rodriguez.** 1988. Isolation and characterization of two plaque size variants of Theiler's murine encephalomyelitis virus (DA strain). J. Gen. Virol. **69:**2413–2418.
63. **Rodriguez, M., L. R. Pease, and C. S. David.** 1986. Immune-mediated injury of virus-infected oligodendrocyte: a model of multiple sclerosis. Immunol. Today **7:**359–363.
64. **Rodriguez, M., E. Oleszak, and J. Leibowitz.** 1987. Theiler's murine encephalomyelitis: a model of demyelination and persistence of virus. Crit. Rev. Immunol. **7:**325–365.
65. **Stuehr, D. J., and C. F. Nathan.** 1989. Nitric oxide. A macrophage product responsible for cytostasis and respiratory inhibition in tumor cells. J. Exp. Med. **169:**1543–1555.
66. **Stuehr, D. J., and O. W. Griffith.** 1992. Mammalian nitric oxide synthases. Adv. Enzymol. Relat. Areas Mol. Biol. **65:**287–346.
67. **Sun, N., D. Grzybicki, R. F. Castro, S. Murphy, and S. Perlman.** 1995. Activation of astrocytes in the spinal cord of mice chronically infected with a neurotropic coronavirus. Virology **213:**482–493.
68. **Theiler, M.** 1937. Spontaneous encephalomyelitis of mice: a new virus disease. J. Exp. Med. **65:**705–719.
69. **Traugott, U., E. L. Reinherz, and C. S. Raine.** 1983. Multiple sclerosis: distribution of T cell subsets within active chronic lesions. Science **219:**308–310.
70. **Tucker, P. C., D. E. Griffin, S. Choi, N. Bui, and S. Wesselingh.** 1996. Inhibition of nitric oxide synthesis increases mortality in Sindbis virus encephalitis. J. Virol. **70:**3972–3977.
71. **Van Dam, A.-M., J. Bauer, W. K. H. Man-A-Hing, C. Marquette, F. J. H. Tilders, and F. Berkenbosch.** 1995. Appearance of inducible nitric oxide synthase in the rat central nervous system after rabies virus infection and during experimental allergic encephalomyelitis but not after peripheral administration of endotoxin. J. Neurosci. Res. **40:**251–260.
72. **Vodovotz, Y., C. Bogdan, J. Paik, Q. W. Xie, and C. Nathan.** 1993. Mechanisms of suppression of macrophage nitric oxide release by transforming growth factor-beta. J. Exp. Med. **178:**605–613.
73. **Wei, X., I. G. Charles, A. Smith, J. Ure, G. Feng, F. Huang, D. Xu, W. Muller, S. Moncada, and F. Y. Liew.** 1996. Altered immune responses in mice lacking inducible nitric oxide synthase. Nature **375:**408–411.
74. **Weinberg, J. B., D. Granger, D. S. Pisetsky, M. F. Seldin, M. A. Misukonis, S. N. Mason, A. M. Pippen, P. Ruiz, E. R. Wood, and G. S. Gilkeson.** 1994. The role of nitric oxide in the pathogenesis of spontaneous murine autoimmune disease: increased nitric oxide production and nitric oxide synthase expression in MRL-Ipr/lpr mice and reduction of spontaneous glomerulonephritis and arthritis by orally administered N^G-monomethyl-L-arginine. J. Exp. Med. **179:**651–660.
75. **Wink, D. A., K. S. Kasprzak, C. M. Maragos, R. K. Elespuru, M. Misra, T. M. Dunams, T. A. Cebula, W. H. Koch, A. W. Andrews, J. S. Allen, and L. K. Keefer.** 1991. DNA deaminating ability and genotoxicity of nitric oxide and its progenitors. Science **254:**1001–1003.
76. **Wink, D. A., and J. Laval.** 1994. The Fpg protein, a DNA repair enzyme, is inhibited by the biomediator nitric oxide *in vitro* and *in vivo*. Carcinogenesis **15:**2125–2129.
77. **Xie, Q. W., H. J. Cho, J. Calaycay, R. A. Mumford, K. M. Swiderek, T. D. Lee, A. Ding, T. Troso, and C. Nathan.** 1992. Cloning and characterization of inducible nitric oxide synthase from mouse macrophages. Science **256:**225–228.
78. **Zielasek, J., M. Tausch, K. V. Toyka, and H. P. Hartung.** 1992. Production of nitrite by neonatal rat microglial cells/brain macrophages. Cell. Immunol. **141:**111–120.